

The Impact of Bound Stellar Orbits and General Relativity on the Temporal Behavior of Tidal Disruption Flares

Lixin Dai

Departamento de Astronomia, Universidad de Chile, Santiago, Chile;

Department of Astronomy, Yale University, New Haven, CT 06511

Andres Escala

Departamento de Astronomia, Universidad de Chile, Santiago, Chile

Paolo Coppi

Department of Astronomy, Yale University, New Haven, CT 06511

`lixin.dai@yale.edu`

Received _____; accepted _____

Preprint

ABSTRACT

We have carried out general relativistic particle simulations of stars tidally disrupted by massive black holes. When a star is disrupted in a bound orbit with moderate eccentricity instead of a parabolic orbit, the temporal behavior of stellar debris changes qualitatively. Stellar debris travels in bound orbits, and returns to the pericenter within a short spread of time, so the fallback rate is much higher than the Eddington rate. Further if the star is disrupted very close to the hole in a regime where general relativity is important, the stellar and the debris orbits display general relativistic precession. Apsidal motion can make the debris stream cross itself after several orbits, which leads to fast dissipation of the debris binding energy. If the star is disrupted in an inclined orbit around a spinning hole, Lense-Thirring precession reduces the probability of such self-crossing, and circularization cannot happen in dynamical timescale. Although we have not computed the light curve using hydrodynamical simulations, examination of dynamics suggests that quasi-periodic flares with small durations, produced by repeated debris pericenter passages, should be exhibited in the early-time light curve. The late-time light curve might still show power-law behavior which is generic to accretions. We suggest that in order to detect these non-standard tidal disruption events in future surveys, the detection triggers should be extended to capture such short-term variations which do not look like standard tidal disruption flares. Also, the initial period of the light curve should be paid more attention as it tells more physics.

Subject headings: accretion, accretion disks — black hole physics — galaxies: nuclei — relativistic processes — stars: kinematics and dynamics

1. Introduction

Tidal disruption (TD) of stars by massive black holes (MBHs) has been theoretically predicted since the 1970s (e.g., Hills 1978; Lacy et al. 1982; Carter & Luminet 1983). The detection of tidal disruption events (TDEs) can be used to probe dormant MBHs in distant galaxies. The tidal disruption of a white dwarf, if ever detected, would be evidence for the existence of intermediate-mass black holes (IMBHs). The earliest observational candidates date back to X-ray flares detected by ROSAT in the 1990s (e.g., Komossa & Bade 1999; Komossa & Greiner 1999). Optical, UV, and X-ray surveys subsequently discovered ~ 20 TD candidates (Gezari et al. 2009; Komossa 2012, and the references therein). Two possible relativistic TD flares have also been detected (e.g., Bloom et al. 2011; Cenko et al. 2012), with X-ray quasi-periodic oscillations (QPOs) reported for the Sw J1644+57 event (Reis et al. 2012). Future time-domain surveys such as using the Large Synoptic Survey Telescope (LSST) are predicted to increase the sample size of TDEs by a factor of 100 in the next decade. In preparation, It is thus important to study the temporal behavior of TD flares, in order to detect TDEs more effectively and gain insight into MBH space-time and accretion physics.

Rees (1988) has presented a general picture of TDEs which is currently used to compare against observations. Here a solar-type star is scattered from faraway into the loss-cone of a massive black hole (MBH). Put the star into a parabolic orbit, if the orbital pericenter distance R_p is closer than the tidal radius R_T , which is defined by the distance where the tidal force from the MBH equals the stellar self-gravity, the star will be torn apart by tidal force in a single flyby. The tidal radius is:

$$R_T = \eta \times R_\star (M/m_\star)^{1/3}, \quad (1)$$

where M is the mass of the MBH, m_\star and R_\star are the stellar mass and radius, and η is a constant of order unity determined by the stellar model (hereafter we take $\eta = 1$). After

disruption, stellar debris initially follows ballistic orbits determined by the distribution of debris binding energy at the time of disruption. Half the debris escapes in hyperbolic orbits, and the other half remains bound to the MBH. If the stellar mass per binding energy, dm/dE , is constant, the rate of debris mass orbiting back to the pericenter (the so called “fallback” rate) goes as a power law with time $\sim t^{-5/3}$ (Phinney 1989; Evans & Kochanek 1989; Lodato et al. 2009). The internal dynamics of the debris including collisions, shear viscosity and shocks eventually leads to the circularization of debris orbits and the formation of an accretion disk (Kochanek 1994). A typical fallback timescale (years) is long compared to the viscous timescale of a standard accretion disk, accretion rate follows the fallback rate, at least at late times (Rees 1988; Ulmer 1999). The result is a luminous electromagnetic flare, likely peaked in the UV/X-rays, which also decays with $t^{-5/3}$ (Strubbe & Quataert 2009; Ayal et al. 2000).

As recognized in Rees (1988), this TD picture has not considered many important factors such as deep encounters (the penetration parameter $\beta = R_T/R_p > 1$), different stellar models, and the change of debris binding energy by tidal compression. The details of the loss of debris angular momentum are also missing. Inclusion of some of these factors can lead to different observational outcomes, as shown, e.g., by Rosswog et al. (2009); Guillochon et al. (2009); Guillochon & Ramirez-Ruiz (2012); Stone et al. (2012). Among these factors, two deserve more study - the parabolic nature of the stellar nature and the effects of general relativity (GR) on the debris orbits:

1. A star is conventionally assumed to be in a parabolic orbit, since it loses energy and angular momentum slowly through many weak scatterings faraway from the hole till it just becomes marginally bound. However, one strong encounter (e.g. with a massive perturber such as a molecular cloud or an IMBH) could remove enough angular momentum to put the star in a bound orbit with $e < 1$ (e is the orbital eccentricity, which equals 1 for

parabolic orbits) (e.g., see Alexander (2012)). Alternatively, a binary stellar system can be tidally separated, so one of the stars remains bound (Amaro-Seoane et al. 2012). A star in such a bound orbit loses angular momentum and energy through gravitational radiation and dynamical frictions with ambient material. After many orbits, R_p could be less than R_T , and the star will be disrupted in an orbit with moderate e .

2. Even in the parabolic case, the star can be disrupted close to the MBH, at a few gravitational radii $R_g = GM/c^2$ (where G is the gravitational constant, and c is the speed of light). If the dimensionless tidal disruption radius

$$\tilde{R}_T = R_T/R_g \propto M^{-2/3} \bar{\rho}_\star^{-1/3}, \quad (2)$$

where $\bar{\rho}_\star$ is the mean stellar density, approaches order unity, GR effects becomes very important. As Fig. 1 shows, the parameter space for such relativistic TD is important. A white dwarf can only be disrupted by IMBHs within $\sim 10R_g$. Higher-mass black holes (a few times of $10^7 M_\odot$ to $10^8 M_\odot$ and even rapidly spinning $10^9 M_\odot$ (Kesden 2012a)) can only disrupt stars if they are in relativistic orbits, unless the star is a giant with an extended envelope (in which case the envelope will be tidally stripped but the dense core will still be disrupted in a close, relativistic orbit).

If a star is disrupted at $\tilde{R}_T < 10$ in a bound orbit, the behaviors of the debris orbits, the circularization mechanism, and the accretion and radiation physics could all be different from the standard scenario. Some of these effects induced by GR or bound orbits have already been studied. Kesden (2012a,b); Haas et al. (2012) calculated some of the features of stars disrupted in GR parabolic orbits. Hayasaki et al. (2012) did hydrodynamical simulations to study a star disrupted in a bound orbit, using a pseudo-Newtonian potential which is a good approximation to the Schwarzschild potential for $e \sim 1$.

In this paper, we extend the previous work by doing the first full GR simulation of a star disrupted in a bound orbit with moderate eccentricity by a spinning MBH without

considering hydrodynamical effects. In section 2, we introduce our code and the set-up of the problem. In section 3, we examine the importance of bound stellar orbits and GR on the initial fate of the tidal debris. Then in the last section, we speculate on the subsequent debris accretion and observational signatures.

2. Methodology

In our simulations we chose a lower main-sequence star with $\sim 0.3M_\odot$ mass with a $10^7 M_\odot$ MBH. Using Eqn. (2), $\tilde{R}_T \sim 7$, in a regime where GR is very important. (The innermost stable circular orbit (ISCO) of the MBH is in the range of $\sim R_g$ (maximally prograde spin) to $9R_g$ (maximally retrograde spin).) We used rejection sampling to generate 10^6 particles with identical masses representing the stellar debris. The geometric distribution of these particles follows the polytropic model with index $\gamma = 5/3$ calculated using Lane-Emden equation.

The star travels in a general relativistic eccentric orbit as one single particle before it is disrupted. There is no closed eccentric orbit in GR, but the orbit can be approximated as an ellipse with apsidal and Lense-Thirring precessions. The eccentricity can be defined by $e = (R_a - R_p)/(R_a + R_p)$, where R_a is the apocenter distance. After disruption, each debris particle travels on its own geodesic calculated using the position and binding energy of the particle at disruption. The effect of tidal compression before disruption and self-gravity are ignored in these simulations. However, as we took $\beta = 1$ in these simulations, tidal compression is not strong near pericenter (Carter & Luminet 1983).

The 5th-order Runge-Kutta algorithm is used to integrate the debris orbits under Schwarzschild or Kerr metric. Our simulation, if running on a single CPU computer, can follow 10^6 debris particles for several orbits with an error of 10^{-11} in only ~ 1 hr. Therefore,

the code is very effective in testing extensive stellar orbital and MBH parameters.

3. Results

3.1. Small spread in fallback time

If a star is disrupted in a bound orbit ($e < 1$), the center of the star has a negative binding energy. Therefore, more than half of the debris remains bound and eventually accretes onto the MBH. If the eccentricity is small enough, even all debris can be bound (Hayasaki et al. 2012). The fallback time of the most bound debris is sensitive to the stellar orbital size and eccentricity. The spread of fallback time, which is the difference between the orbital time of the most loosely and tightly bound debris, greatly shortens as e decreases.

We simulated the debris orbits from a star disrupted by a $10^7 M_\odot$ Schwarzschild black hole. As we keep the same $R_p = R_T \sim 7R_g$ but change e , it can be seen in Fig. 2 that the mostly bound debris comes back sooner as e decreases. Also, the spread of fallback time decreases from ~ 1 year (in the parabolic case) to weeks ($e = 0.99$), days ($e = 0.9$), or even hours ($e = 0.7$). As a result, if a star is disrupted in an orbit with moderate eccentricity, the mass fallback rate is very high, and it does not decay as $t^{-5/3}$.

Although the mass fallback rate is huge, it is uncertain how much mass will circularize as debris returns to the pericenter. Kochanek (1994) discussed different mechanisms (including collisions between debris streams, shear stress, shocks, and tidal compression) that can dissipate the debris energy. When the star is disrupted in a parabolic orbit, these mechanisms are effective, since the debris can collide at a big angle due to the large dispersion in the debris orbital time - as the loosely bound debris returns to pericenter for the first time, more tightly bound debris has already travelled several orbits with GR precession. However, if a star is disrupted in an orbit with moderate e , the debris travels

and returns to the pericenter almost together, so the collisions and shear stress between debris should be weak. Also as debris does not travel very far from the hole, the expansion and vertical compression of the debris should not be strong either. A hydrodynamical simulation similar to Ramirez-Ruiz & Rosswog (2009) needs to be done to check the circularization rate, but it is quite likely that the previously discussed mechanisms are not effective in dissipating debris energy in this case. However, another mechanism, namely the self-crossing of the debris stream, could be the major mechanism for debris energy dissipation, as we will discuss in section 3.2.

3.2. Self-crossings of the debris stream

The debris orbit has two types of GR precession: apsidal motion and Lense-Thirring precession. Apsidal motion is the advance of the pericenter on the orbital plane. After debris traces out several orbits, the debris stream is tangentially elongated. At the pericenter where apsidal motion is strong, the “head” of the debris stream can catch its “tail” if the stream is long enough. We show in Fig. 3 that such self-crossing happens in the 9th orbit, after a lower main-sequence star is disrupted in an $e = 0.7$ orbit around a $10^7 M_\odot$ Schwarzschild hole. If the same star is disrupted in an orbit with $e = 0.9$ (R_p the same), self-crossing can even happen in the first orbit. Therefore, if we increase the eccentricity, or decrease the orbital size, apsidal motion is more prominent, and the possibility of self-crossing happening increases.

As we can see in the Fig. 3, when self-crossing happens, the colliding angle between debris can be within $90^\circ - 180^\circ$. Therefore, strong energy dissipation due to heating and shocks makes debris lose angular momentum and energy in fast, dynamical timescale. We compared our ballistic debris orbits with the orbits with hydrodynamical effects considered in Hayasaki et al. (2012), and found that there is no significant deviation until self-crossing

happens. This confirms that self-crossing is the main mechanism for circularizing debris in such orbits in dynamical timescale. If we assume a standard accretion disk is formed, the viscous timescale will be much longer than the circularization timescale, which is a few times of the orbital periods. This means that the debris will accumulate and probably form a thick disk, with accretion rate not following the fallback rate.

In nature MBHs are likely to be spinning, and there is no reason to assume that stars approach in equatorial orbits. Lense-Thirring effect needs to be considered to address the precession of the orbital plane when debris travels in inclined orbits. Fig. 4 shows that if a star is disrupted in an inclined orbit around a fastly spinning hole, self-crossing will not happen in dynamical timescale. With hydrodynamical effects, the debris stream will expand, so the “head” and “tail” of the stream might still have some interaction, but this interaction will be much weaker than the strong collision in the equatorial case. Therefore, debris circularizes much more slowly around a spinning hole.

With the advance of the pericenter on the orbital plane and the precession of the orbital plane itself, debris passes pericenter at different azimuthal and inclination angles. After many orbits, the debris will form a thick shell of gas around the hole. Accretion from such a thick shell could be slow if there is no other mechanism for energy and angular momentum dissipation. It is worthwhile to conduct hydrodynamical simulations to study such an accretion scenario.

3.3. Quasi-periodic flares

Before most of the debris circularizes, each time the debris stream passes the pericenter, a short flare might be produced due to dissipation of debris energy, especially if self-crossing happens. If the star is disrupted in a general relativistic eccentric orbit, these flares will be

produced quasi-periodically. The short flares are separated by $P \sim$ the original stellar radial orbital period, which depends on the eccentricity, size and inclination of the stellar orbit, and the spin of the MBH. Therefore, if such QPOs are observed, they could in principle be used to constrain these parameters.

Fig 5. shows how much mass enters the tidal radius with time, assuming no circularization. With hydrodynamical effect, some fraction of debris will circularize at pericenter passages, and the energy profile of the debris will flatten faster, but some QPO features should still be preserved.

4. Discussion

In conclusion, if a star is tidally disrupted in a bound orbit with moderate eccentricity very close to a MBH, all the debris remains bound, and returns to the pericenter in a spread of time much shorter than the typical fallback time of a star disrupted in a parabolic orbit. The fallback rate is super-Eddington, and does not decay as $t^{-5/3}$. It is hard for the debris to lose energy unless self-crossing of the debris stream can happen due to apsidal motion. However, in nature Lense-Thirring effect will reduce hydrodynamical interactions, and a thick shell of gas without rapid accretion is likely to be formed around the MBH.

Hydrodynamical simulations need to be conducted to calculate the debris circularization and accretion rate and the exact shape of the light curve. The total duration of the flare could be shorter than years, but this also depends on the accretion model. The flare light curve in the late time might still exhibit some power-law behavior, which is a generic feature of accretions. However, in the early time, the light curve is likely to be very different. Peaks with short durations ($\sim 1 - 10$ hours) imprinted by the spread of debris fallback time could be observed quasi-periodically with P ($\sim 1 - 10$ days) determined by the stellar

orbit. Lense-Thirring effect lowers the magnitude of these short peaks, but also gives the sensitivity of probing the space-time around black holes. Therefore, the early-time TD light curve contains more information on the MBH and stellar orbital parameters and the accretion physics, and thus should be monitored more closely.

The TD of a star in a bound orbit close to the MBH will likely to be observed in the next decade, as the launch of LSST and other telescopes will greatly enlarge the TDE sample size. It is very useful to study the temporal behavior of such non-standard TD flares more carefully using hydrodynamical simulations, and extend the trigger in future surveys to cover such short flares which do not look like standard TD flares. The rate of such TDEs might be low, but the observation of even just one or two of them can greatly improve our understanding on the dynamics and accretion around MBHs.

We are grateful to Roger Blandford and Priya Natarajan for discussions and encouragement. The stellar model is kindly provided by Peter Eggleton. We would also like to thank Pau Amaro-Seoane, Xian Chen, Michael Kesden, Jonathan McKinney, Cole Miller, Gabe Perez-Giz, Nick Stone, and Alexander Tchekhovskoy for useful conversations. L.D. acknowledges the support from the Financiamiento Basal Grant PFB 06 and the Yale-Universidad de Chile Joint Program. A.E. acknowledges partial support from the Financiamiento Basal Grant PFB 06, FONDECYT Grant 1130458 and Anillo de Ciencia y Tecnologia Grant ACT1101.

REFERENCES

- Alexander, T. 2012, European Physical Journal Web of Conferences, 39, 5001
- Amaro-Seoane, P., Miller, M. C., & Kennedy, G. F. 2012, MNRAS, 425, 2401
- Ayal S., Livio M., Piran T., 2000, ApJ, 545, 772
- Bardeen, J. M., & Petterson, J. A. 1975, ApJ, 195, L65
- Bloom J. S., Giannios D., Metzger B. D., et. al., 2011, Science, 333, 203
- Burrows D. N., Kennea J. A., Ghisellini G., et. al., 2011, Nature, 476, 421
- Carter B., Luminet J.-P., 1983, A&A, 121, 97
- Cenko S. B., Krimm H. A., Horesh A., et. al., 2012, ApJ, 753, 77
- Dai L. J., Fuerst S. V., Blandford R., 2010, MNRAS, 402, 1614
- Evans C. R., Kochanek C. S., 1989, ApJ, 346, L13
- Gezari S., Heckman T., Cenko S. B., Eracleous M., Forster K., Gonçalves T. S., Martin D. C., Morrissey P., Neff S. G., Seibert M., Schiminovich D., Wyder T. K., 2009, ApJ, 698, 1367
- Gezari S., Chornock R., Rest A., et. al., 2012, Nature, 485, 217
- Guillochon J., Ramirez-Ruiz E., Rosswog S., Kasen D., 2009, ApJ, 705, 844
- Guillochon, J., & Ramirez-Ruiz, E. 2012, arXiv:1206.2350
- Haas R., Shcherbakov R. V., Bode T., Laguna P., 2012, ApJ, 749, 117
- Hayasaki, K., Stone, N., & Loeb, A. 2012, arXiv:1210.1333

- Hills, J. G. 1978, MNRAS, 182, 517
- Kesden M., 2012a, Phys. Rev. D, 86, 064026
- Kesden M., 2012b, Phys. Rev. D, 85, 024037
- Kochanek, C. S. 1994, ApJ, 422, 508
- Komossa S., Bade N., 1999, A&A, 343, 775
- Komossa S., Greiner J., 1999, A&A, 349, L45
- Komossa, S. 2012, European Physical Journal Web of Conferences, 39, 2001
- Lacy, J. H., Townes, C. H., & Hollenbach, D. J. 1982, ApJ, 262, 120
- Lodato G., King A. R., Pringle J. E., 2009, MNRAS, 392, 332
- Phinney E. S., 1989, in Morris M., ed., The Center of the Galaxy Vol. 136 of IAU
Symposium, Manifestations of a Massive Black Hole in the Galactic Center. p. 543
- Ramirez-Ruiz, E., & Rosswog, S. 2009, ApJ, 697, L77
- Rees M. J., 1988, Nature, 333, 523
- Reis R. C., Miller J. M., Reynolds M. T., Gültekin K., Maitra D., King A. L., Strohmayer
T. E., 2012, Science, 337, 949
- Rosswog S., Ramirez-Ruiz E., Hix W. R., 2009, ApJ, 695, 404
- Stone, N., Sari, R., & Loeb, A. 2012, arXiv:1210.3374
- Strubbe L. E., Quataert E., 2009, MNRAS, 400, 2070
- Ulmer, A. 1999, ApJ, 514, 180

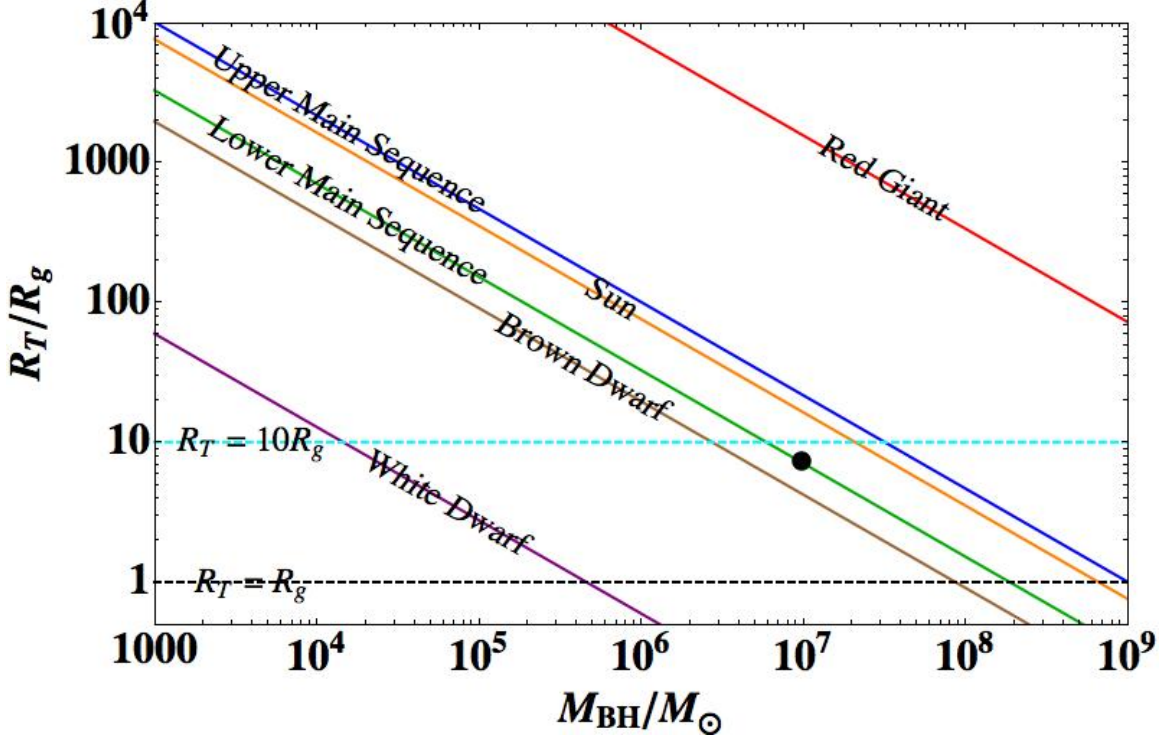


Fig. 1.— The dimensionless tidal disruption radius of different stars around MBHs with different masses. Here we adopted Peter Eggleton’s simulations to calculate the typical stellar density of different types of stars: a Sun-like star (yellow), a lower main sequence dwarf star with a mass $\sim 0.3M_\odot$ (green), an upper main sequence star with a mass $\sim 7.9M_\odot$ (blue), a red giant with a mass $\sim 7.1M_\odot$ (orange), a white dwarf with a mass $0.8M_\odot$ (purple), and a brown dwarf with a mass $0.05M_\odot$ (brown). The black dashed horizontal corresponds to the gravitational radius, which is a lower bound of the event horizon. The cyan dashed line corresponds to 10 gravitational radius, below which GR is important. The lower main-sequence star has a tidal radius at $\sim 7R_g$ when encountering a 10^7M_\odot MBH, as marked by the black dot.

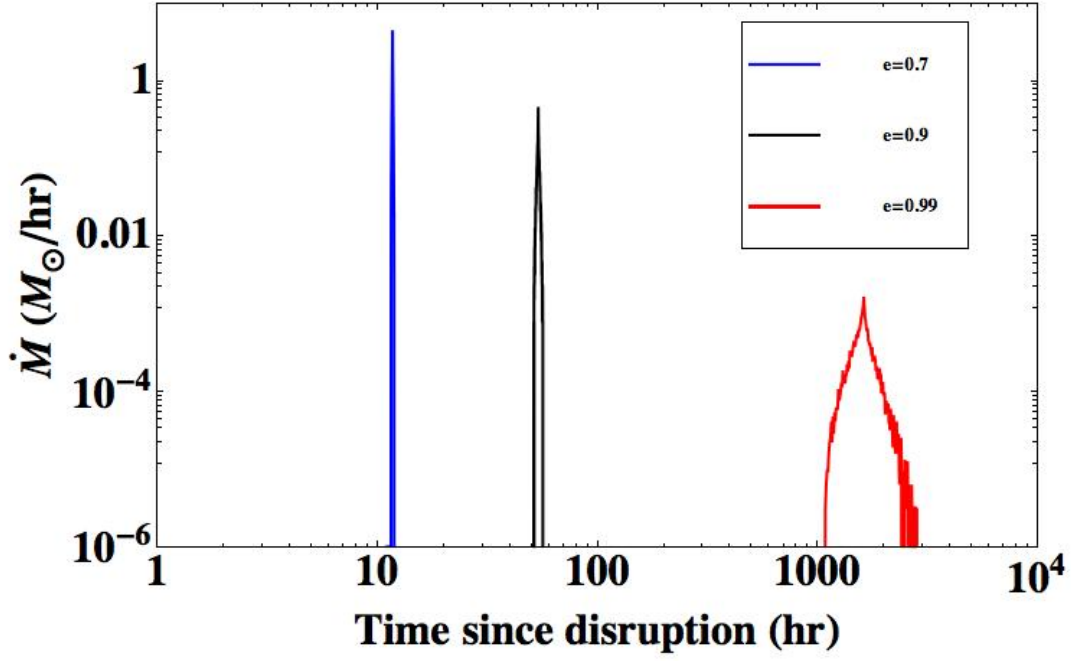


Fig. 2.— The fallback rate as a function of time after disruption for a $\sim 0.3M_\odot$ dwarf star disrupted by a 10^7M_\odot Schwarzschild MBH. The star is put in bound orbits with the same R_p but different eccentricities. This rate shows how much time it takes the debris to return to pericenter for the first time after disruption, with no hydrodynamical effect. The spread of the fallback time and peak fallback rate are very sensitive the to the orbital eccentricity.

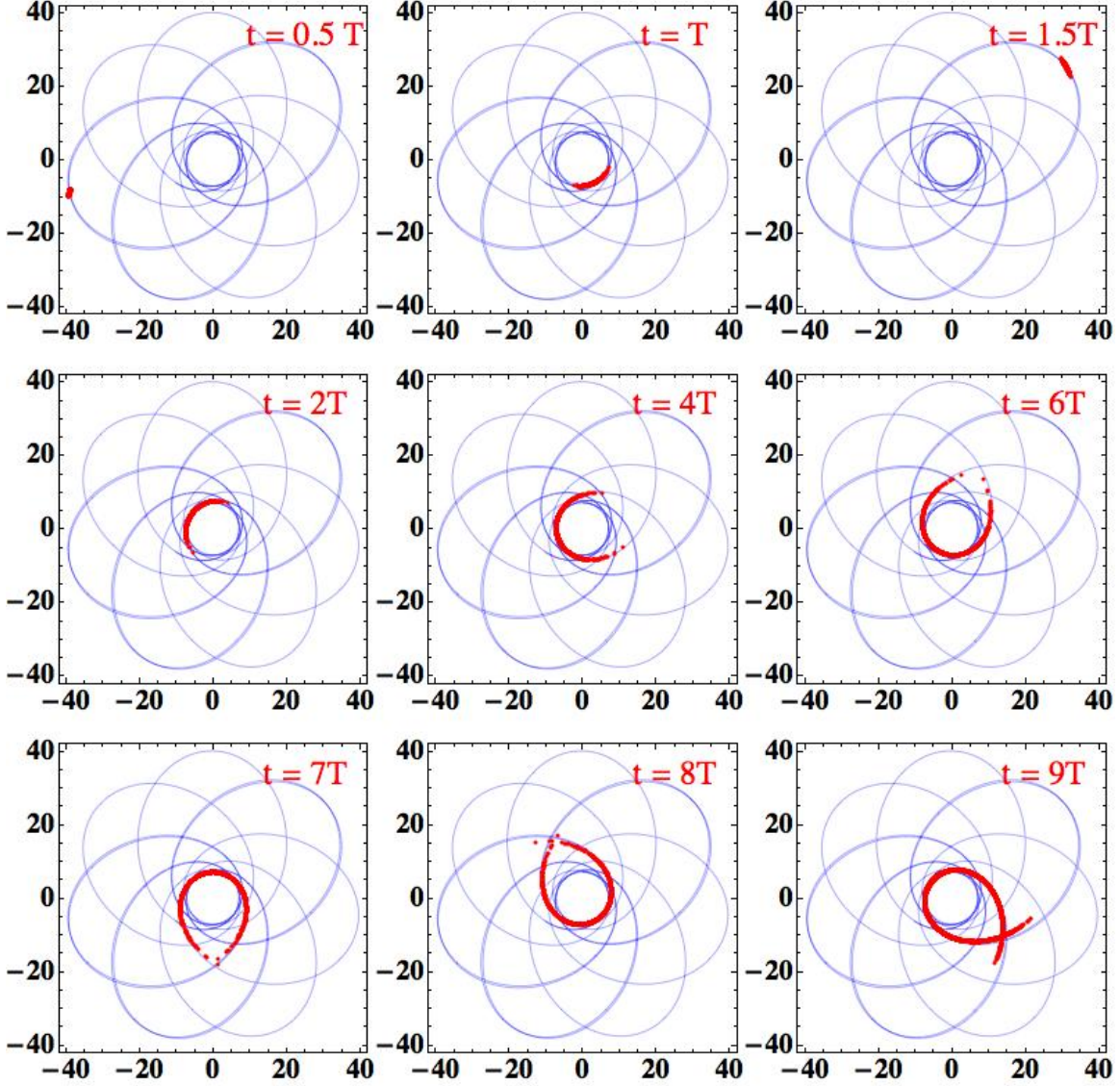


Fig. 3.— The snapshots of the debris stream of a $\sim 0.3M_{\odot}$ lower main-sequence star disrupted by a Schwarzschild 10^7M_{\odot} black hole. The original stellar orbit is an ellipse with $e = 0.7$ with $R_p \sim 7R_g$ and $R_a \sim 40R_g$, as represented by the blue curve. The MBH is at the center. The red points represent the positions of debris particles traveling on the equatorial plane at different epochs. T is the orbital time of the original stellar orbit, so at $t = T/2$ the debris goes to the apocenter for the first time and at $t = T$ the debris returns to the pericenter for the first time. The debris stream elongates as it orbits around the black hole. In the 9th orbit, the stream is long enough to cross itself at the pericenter.

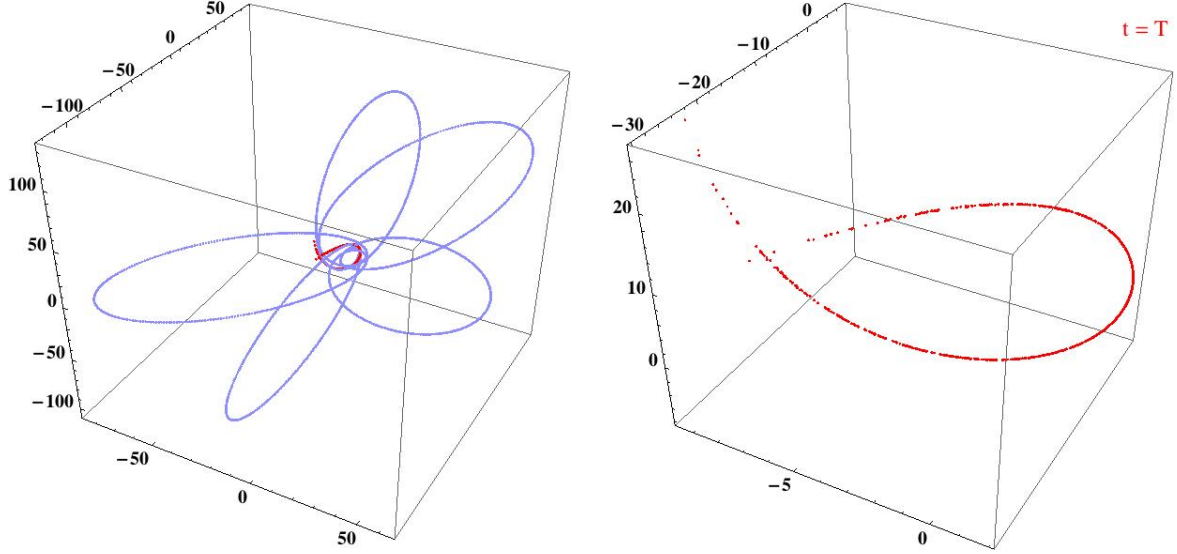


Fig. 4.— The debris stream of a $\sim 0.3M_{\odot}$ dwarf star disrupted in a highly inclined orbit by a Kerr 10^7M_{\odot} black hole with spin parameter 0.5. Left panel: The vertical direction is the MBH spinning axis direction. The star is disrupted at $R_p \sim 7R_g$ of an eccentric orbit with $e = 0.9$ and close to 90° inclination angle. The blue curve is the orbit of the star if it is not disrupted. The red points represent the locations of debris particles when they pass by the pericenter for the first time. Right panel: The debris stream would have crossed itself in the first orbit if the MBH had no spin or the stellar orbit was equatorial, but here self-crossing does not happen due to the frame-dragging of the orbital plane.

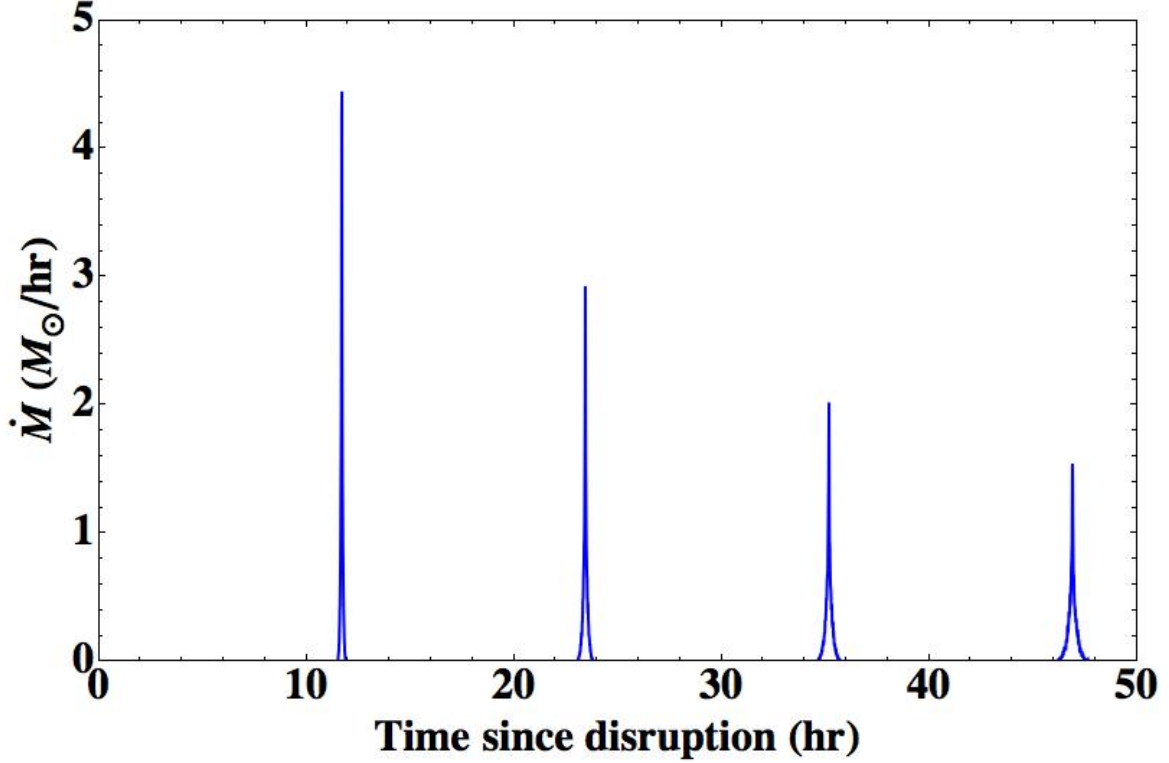


Fig. 5.— The rate of the debris mass entering the tidal radius, after the disruption of a star in an eccentric orbit with the same set-up as in Fig. 2. Here it is assumed that no hydrodynamical effects happen, so the debris just orbits the hole without any mass loss. It can be seen that the debris particles move together and pass the pericenter in a short duration. Quasi-periodic flares might be produced from repeated pericenter passages. The period is roughly the same as the original stellar radial orbital period. In this figure, the peak rate drops and duration of flare increases at each passage, purely due to dynamical effects.